ADAPTIVE STEPSIZE CONTROL STRATEGIES IN FINITE ELEMENT SIMULATION OF 2D RAYLEIGH-BENARD-MARANGONI FLOWS

Andréa M.P. Valli
Álvaro L.G.A. Coutinho
Universidade Federal do Rio de Janeiro, Departamento de Engenharia Civil
Cx. P.68506 - Rio de Janeiro, RJ 21945-970, Brazil
Graham F. Carey
The University of Texas at Austin, CFD Lab
ASE/EM Dept., WRW 301 - Austin, TX 78712, USA

Abstract. Natural convection of an incompressible fluid can be driven by buoyancy forces due to temperature gradients and thermocapillary forces caused by gradients in the surface tension. These flows, termed Rayleigh-Benard-Marangoni problems, are of great interest in studying pattern formation in hydrodynamical systems. A decoupled finite element formulation with adaptive feedback control for timestep selection has been developed for 2D viscous flow problems involving heat transfer and surface tension effects. The finite element flow formulation is based on a penalty Galerkin method and the heat equation utilizes a Galerkin approach. Representative Rayleigh-Benard and Marangoni flow calculations are presented, and the efficiency of the present timestep scheme is examined and compared with other time-stepping strategy.

Keywords: Rayleigh-Benard-Marangoni flows, adaptive feedback control, timestep selection, finite element

1. INTRODUCTION

Coupled viscous flow and heat transfer computations are of great interest in studying pattern formation in hydrodynamical systems. Practical applications include, for example, pattern formation during solidification, welding in manufacturing processes and growth phenomena to defect fracture and crack propagation. Rayleigh-Benard-Marangoni problems become very popular as prototypes of complex behavior where nonlinear theories of pattern formation may be tested. Recently, special attention has been paid to the study and implementation of numerical and computational techniques to develop effective

algorithms capable of high resolution 3D viscous flows involving heat transfer and surface tension effects. For example, domain decomposition strategies and parallel gradient-type iterative solution schemes have been developed and implemented with success for 3-D Rayleigh-Benard-Marangoni flow calculations [1]. These techniques permit making fundamental phenomenological flow studies at the grid resolution necessary to represent the fine scale surface-driven phenomena. Several adaptive timestepping selection strategies have been also studied as a means to provide stable accurate transient (and steady state) solutions more efficiently [8, 9].

The focus in our work is the use of a control approach for automatic timestep selection for solving 2D coupled viscous flow and heat transfer computations. Adaptive techniques for automatic timestep determination are usually based on approximate local truncation error measures or on purely heuristic considerations. Winget and Hughes, [9], develop step size selections based on heuristic rules for transient heat conduction. We remark that adaptive timestep selection can be viewed as an example of a feedback control problem, [6, 7].

The equations describing 2D Rayleigh-Benard-Marangoni flows are the coupled incompressible Navier Stokes and heat transfer equations. The present algorithm employs a decoupled scheme, where the momentum and continuity equations are solved first, in each timestep, lagging the temperature in the forcing term. Then, the heat transfer equation is solved with the computed velocities as input. The finite element flow formulation is based on a penalty Galerkin method to enforce the incompressibility constraint, and the heat equation utilizes a Galerkin approach. Spatial discretization of the Navier Stokes equations gives rise to a semi-discrete ODE system for the velocities that are usually solved by an implicit method. An adaptive timestep selection scheme is central to an efficient numerical integration of the ODE equations.

The outline of the treatment is as follows. In the next section we briefly state the equations of the 2D Rayleigh-Benard-Marangoni problem, the finite element formulation, and solution approach. Then, we describe a simple PID control approach and indicate how it can be applied to timestep selection of coupled viscous flow and heat transfer computations. Next, results of the classic Rayleigh-Benard problem and Rayleigh-Benard-Marangoni problem are compared for fixed timestep, an adaptive timestep scheme in the literature and our PID control approach.

2. FORMULATION AND APPROXIMATION

Natural convection of an incompressible fluid can be driven by buoyancy forces due to temperature gradients and thermocapillary forces caused by gradients in the surface tension. When a thin horizontal layer fluid between two horizontal plates is heated from below, a temperature gradient is generated across the plates. At critical Rayleigh number, circular convection cells set in - the heated fluid near the bottom begins to rise while the cooler fluid near to the top descends. Buoyancy is a dominant component in driving this type of flow termed Rayleigh-Benard problem. If the plate is removed from the upper surface, then the surface tension effects associate with temperature gradients on the free surface become important. Now both buoyancy and thermocapillary effects provide the

dominant forces driving the flow for this classical Rayleigh-Benard-Marangoni problem.

We consider the transient flow of viscous incompressible fluid as described by the Navier-Stokes equations coupled to the heat transfer (energy) equation. Here we confine the study to two-dimensional flows with non-deforming free surface. The dimensionless equations describing the Rayleigh-Benard-Marangoni flows are

$$\frac{\partial \mathbf{u}}{\partial t} + \mathbf{u} \cdot \nabla \mathbf{u} - \Delta \mathbf{u} + \nabla p = -\frac{Ra}{Pr}T\mathbf{g} \qquad \text{in } \Omega \qquad (1)$$

$$\nabla \cdot \mathbf{u} = 0 \qquad \text{in } \Omega \qquad (2)$$

$$\frac{\partial T}{\partial t} + \mathbf{u} \cdot \nabla T - \frac{1}{Pr}\nabla^2 T = 0 \qquad \text{in } \Omega \qquad (3)$$

where $\mathbf{u}$ is the velocity, p is the pressure, T is the temperature, $Ra = \frac{\beta \Delta T g L^3}{\nu \alpha}$ is the Rayleigh number, $Pr = \frac{\nu}{\alpha}$ is the Prandtl number, β is the thermal coefficient, ΔT is the temperature difference for flows with heated or cooled walls, $\mathbf{g}$ is the gravity vector, L is a characteristic length scale of the flow, ν is the kinematic viscosity, and α is the thermal diffusivity.

The boundary conditions are as follows: $\mathbf{u} = \mathbf{u}_w$ (no slip) on $\partial \Omega_1$, $T = T_1(x, y)$ (isothermal boundary) or $\frac{\partial T}{\partial n} = 0$ (adiabatic boundary) on $\partial \Omega_1$, where $\partial \Omega_1$ is the part of the boundary which is not a free surface. On the free surface $\partial \Omega_2$, the shear stress is equal to the gradient in the surface tension σ. We assume that σ varies linearly with T, so $\sigma_T = \frac{\partial \sigma}{\partial T}$ is a constant for a given fluid. The non-dimensional boundary condition on the free surface becomes $\frac{\partial u}{\partial y} = \frac{Ma}{Pr}\frac{\partial T}{\partial x}$, where $Ma = \frac{\sigma_T \Delta T L}{\rho \nu \alpha}$ is the Marangoni number and ρ is the density. Equations (1), (2) and (3) constitute a coupled system of equations to be solved for velocity, pressure and temperature.

The present algorithm employs a decoupled scheme, where the Navier-Stokes equations are solved first, in each timestep, lagging the temperature in the forcing term. Then the temperature is calculated, with the velocities as input. The finite element flow formulation is based on a penalty Galerkin method to enforce the incompressibility constraint, and the heat equation utilizes a Galerkin approach.

Introducing a finite element discretization and basis on Ω_h the variational boundary value problem reduces to find $\mathbf{u}_h \in V^h$ satisfying the initial condition with $\mathbf{u}_h = \mathbf{u}_w$ on $\partial \Omega_1$ such that

$$\int_{\Omega_h} (\frac{\partial \mathbf{u}_h}{\partial t} \cdot \mathbf{v}_h + \nabla \mathbf{u}_h : \nabla \mathbf{v}_h + (\mathbf{u}_h \cdot \nabla)\mathbf{u}_h \cdot \mathbf{v}_h) \, dx \qquad (4)$$

$$+ \frac{1}{\epsilon}\mathbf{I}(\nabla \cdot \mathbf{u}_h)(\nabla \cdot \mathbf{v}_h) \, dx + \int_{\partial \Omega_{2h}} \frac{Ma}{Pr}\nabla T \cdot \mathbf{v}_h ds$$

$$= -\int_{\Omega_h} \frac{Ra}{Pr}T\mathbf{g} \cdot \mathbf{v}_h \, dx \quad \text{for all } \mathbf{v}_h \in V^h \qquad (5)$$

where $\mathbf{I}$ denotes the usual reduced numerical integration for the penalty term. This leads to the following non-linear semidiscrete system of ordinary differential equations

$$\bar{\mathbf{M}}\frac{d\mathbf{u}^*}{dt} + \bar{\mathbf{A}}\mathbf{u}^* + \mathbf{C}(\mathbf{u}^*) + \frac{1}{\epsilon}\bar{\mathbf{B}}\mathbf{u}^* = \bar{\mathbf{F}} \qquad (6)$$

which is linearized by successive approximations and integrated implicitly using a Crank-Nicolson scheme. The solution of the linear systems are obtained using a frontal solver.

To find approximate solutions for the transport problem corresponding to (3), we use a traditional Galerkin finite element formulation. A week variational statement may be obtained by integration by parts of the diffusion term in a standard residual formulation, and then using the Gauss divergent theorem. Assuming that convective and diffusive effects are of same order, we may construct a semidiscrete Galerkin finite element method introducing a spatial discretization and an appropriate finite element space for the admissible functions. The finite element problem is to find $T_h \in {H_0}^h$ satisfying the initial condition such that

$$\int_{\Omega_h} \left(\frac{\partial T_h}{\partial t} \omega_h + \mathbf{u} \cdot \nabla T_h \, \omega_h + \frac{1}{Pr} \nabla T_h \cdot \nabla \omega_h \right) dx = 0 \tag{7}$$

for all $\omega_h \in {H_0}^h$. The resulting semi-discrete ODE system for the nodal vector $\mathbf{T}$ has the form

$$\mathbf{M} \frac{d\mathbf{T}}{dt} + \mathbf{B(u)}\,\mathbf{T} + \mathbf{D}\,\mathbf{T} = 0 \tag{8}$$

We integrate the ODE system implicitly using a Crank-Nicolson scheme. At each timestep we solve a linear system using a frontal solver.

3. ADAPTIVE CONTROL

Control can be defined as the process of making a system of variables follow a particular value, called the reference value. Closed-loop process control uses a measurement of the controlled variable and feedback of this signal to compare it with a reference value. The feedback is supplied from an output sensor of some sort, and feeds an input of the controller to tell the controller how far the output is from its reference value. The controller uses this information to correct the output error.

One of the most widely used algorithms for closed-loop control is the three-term control, known as the Proportional-Integral-Differential (PID) control loop. The popularity of PID controllers can be attributed to their functional simplicity and to their robust performance in a large range of operating conditions. The objective in using PID control algorithms is to control the output along a smooth curve (vs. time) towards the set-point while minimizing overshoot, the amount the system output response proceeds beyond the desired response. According to Hairer and Wanner [7], stepsize selection can be viewed as an automatic control problem with a PID controller defined as

$$\triangle t_{n+1} = \left(\frac{e_{n-1}}{e_n} \right)^{k_P} \left(\frac{tol}{e_n} \right)^{k_I} \left(\frac{e_{n-1}^2}{e_n e_{n-2}} \right)^{k_D} \triangle t_n, \tag{9}$$

where tol is some input tolerance, e_n is the measure of the change of the quantities of interest in time step $\triangle t_n$, and k_P, k_I and k_D are the PID parameters.

An estimate of the solution change is compared with the specified accuracy requirement, and the result is fed back to calculate the new time step. The controller tries to select the stepsize such that e_n comes as close as possible to the input tolerance, tol, along

a smooth curve. The measure of the change over a timestep of the quantities of interest, e_n, is defined by

$$e_n = \max(e_u, e_T)$$

where

$$
\begin{aligned}
e_u &= \frac{\hat{e}_u}{tol_u} \text{ with } \hat{e}_u = \frac{\|\mathbf{u}_{m+1}^* - \mathbf{u}_m^*\|}{\|\mathbf{u}_{m+1}^*\|} \\
e_u &= \frac{\hat{e}_T}{tol_T} \text{ with } \hat{e}_T = \frac{\|\mathbf{T}_{m+1} - \mathbf{T}_m\|}{\|\mathbf{T}_{m+1}\|}
\end{aligned}
$$

Here e_u and e_T are respectively the normalized changes in nodal velocities and temperatures, and $\| \cdot \|$ denotes the Euclidean norm. The corresponding user supplied tolerances are tol_u and tol_T. We supply timestep limits, $(\triangle t)_{min}$ and $(\triangle t)_{max}$, to incorporating the anti_windup effect.

At each timestep, the velocities are calculated with the temperatures as input in the forcing term, and then the temperatures are obtained using the updated velocities. The new timestep size is given by (9), and the velocities and temperature are updated to calculated the new solutions.

If a timestep gives an unacceptable value of e_n, the step is rejected. Then the step is repeated with a scaled timestep size based on the magnitude of the error relative to the tolerance, [8]. However, we find in numerical experiments that the number of rejections is very small, producing a smooth sequence of timesteps. In our algorithm, if the sequence of iterates of the nonlinear system is converging at a slow rate, the timestep is also rejected.

4. NUMERICAL RESULTS

Our first example involves natural convection in a unit square with heated lateral walls and adiabatic top and bottom wall. The computed Nusselt number at the left wall ($Nu_0 = \int_0^1 q dy$, where q is the heat flux), and the stream function at the midpoint (ψ_{mid}) are compared to the results from [2, 3, 4]. Consider the two-dimensional flow of a Boussinesq fluid of $Pr = 0.71$ and $Ra = 10^3$ in an square cavity described by $0 \leq x, y \leq 1$. Both components of the velocity are zero on all the boundaries, the boundaries at $y = 0$ and 1 are insulated, $\frac{\partial T}{\partial y} = 0$, and $T = 1$ at $x = 0$ and $T = 0$ at $x = 1$.

The approximate velocities and temperature are calculated using biquadratic elements in a uniform mesh with size $h = \frac{1}{16}$, a fixed timestep of 0.01, the PID timestep size control, and the Winget and Hughes approach [9]. We assume that the steady-state occurs when $\|\mathbf{u}_{m+1} - \mathbf{u}_m\| < \tau_u \|\mathbf{u}_{m+1}\|$ and $\|\mathbf{T}_{m+1} - \mathbf{T}_m\| < \tau_T \|\mathbf{T}_{m+1}\|$, where m denotes the timestep index, $\| \cdot \|$ denotes Euclidean norm, and τ_u and τ_T are input tolerances. The results are shown in Table 1, and the agreement for all cases are good. The contours of the stream function and temperature are shown in Figures 1. The stream function contour shows the concentric nature of the streamlines.

We compare approximate solutions using a fixed timestep size of 0.01, the PID timestep size control, and Winget and Hughes approach. We start with a timestep size of 0.01, and we allow minimum and maximum timesteps of 0.01 and 0.5, respectively. It is important to note that for step sizes greater than 0.01 the successive iterations failed to converge

Table 1: Comparison of specific results to benchmark case

Fixed Δt		PID control		Winget & Hughes		Benchmark	
Nu_0	ψ_{mid}	Nu_0	ψ_{mid}	Nu_0	ψ_{mid}	Nu_0	ψ_{mid}
1.1184	1.1747	1.1178	1.1740	1.1187	1.1749	1.117	1.174
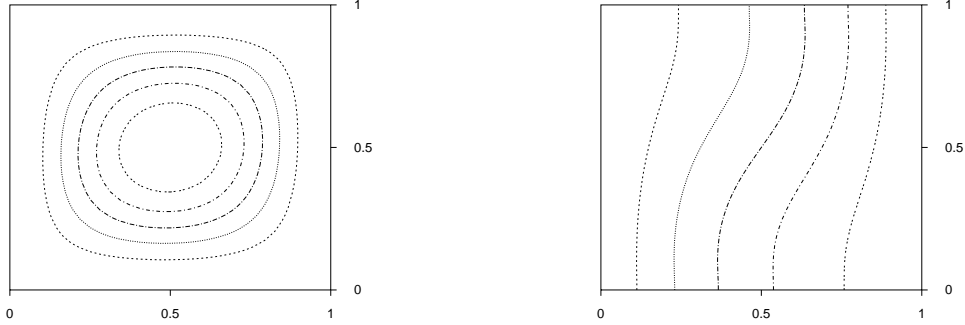
Figure 1: Stream function contours (left) and temperature contour (right) for $Ra = 10^3$ and $Pr = 0.71$

after a few timesteps. The steady-state solutions are obtained at $\tau_u = \tau_T = 10^{-03}$. We define a tolerance of 0.18 for changes in nodal velocities and 0.1 for changes in nodal temperature. The PID parameters are $k_p = 0.075$, $k_i = 0.175$ and $k_d = 0.01$.

Table 2 shows the number of time iterations, $ntstep$, the number of rejected steps, $nrejec$, the total number of successive approximations, nsa, and the computational effort, c_{effort}, defined here as nsa diveded by the number of sucessive approximations obtained using a fixed timestep size. We obtain the solution with 29 successive approximation iterations using the PID controller, and we need 64 iterations with a fixed timestep of 0.01. Thus, we are able to calculate the solution 2.2 times faster using the timestep size control without any significant loss of accuracy. The approach of Winget and Hughes also shows good results for this particular example. Figures 2 shows the timestep size against time using the PID controller and the Winget and Hughes approach. The PID control produce a smooth sequence of timesteps.

Table 2: Results for the natural convection problem with $Ra = 10^3$ and $Pr = 0.71$.

$Ra = 10^3$	$ntstep$	$nrejec$	nsa	c_{effort}
Fixed Δt	27	0	64	1
PID Control	10	0	29	0.45
Winget & Hughes	15	0	40	0.63

In the second example, we consider flow in a rectangular container of length 4 times the height with $Pr = 0.72$ and $Ra = 30000$. The temperatures on the bottom surface and top surface are $T_h = 1$ and $T_c = 0$, respectively. The approximate velocity and temperature are calculated using biquadratic shape functions with a grid of 32×8 elements, and the
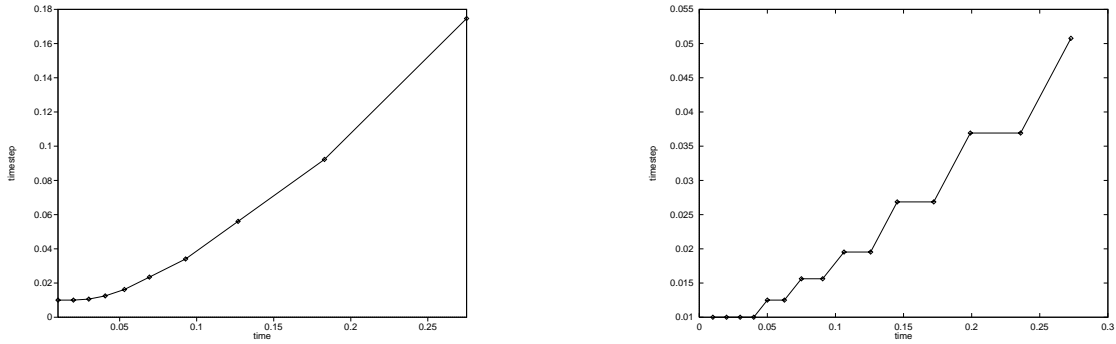
Figure 2: Timestep variation using the PID controller (left) and Winget and Hughes approach (right), $Ra = 10^3$ and $Pr = 0.71$.

PID timestep selection. We consider the steady-state problem and the computed stream function and temperature contours are shown in Figure 3. There are six recirculation cells, and the results agree with those in [5].
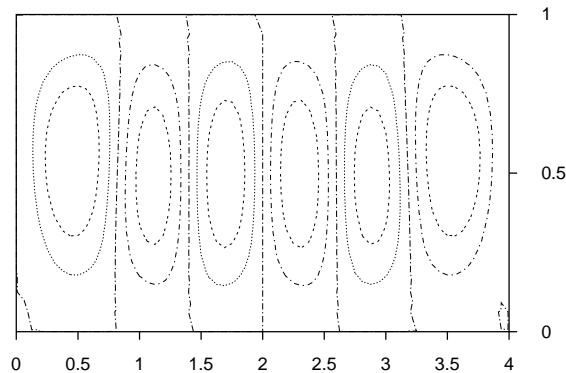

Figure 3: Stream function contour $Pr = 0.72$, $Ra = 30000$ in a container with aspect ratio 4:1

The steady-state solution is obtained at $\tau_u = \tau_T = 10^{-03}$, and we set a tolerance of 0.01 for changes in nodal velocities and temperature. We start with a timestep size of 0.001, and we allow minimum and maximum time steps of 0.001 and 0.5, respectively. This starting timestep is the largest for which we obtained convergence in the successive iterations. The PID parameters are $k_p = 0.075$, $k_i = 0.175$ and $k_d = 0.01$. As we can see in Table 3, we obtain the solutions with 983 successive approximation iterations using the PID controller. With a fixed timestep size of 0.001, we need 1547 iterations. Thus, the solutions are obtained 1.6 times faster using the PID controller. In this problem the PID control also shows better results than the approach used by Winget and Hughes. Figures 4 shows the timestep size against time using the PID controller and the Winget and Hughes approach, respectively.

The third numerical experiment involves buoyancy forces due to temperature gradients and thermocapillary forces caused by gradients in the surface tension. The flow domain and boundary conditions are the same as the first example except that the top is now a

Table 3: Results for the problem using the PID control and the fixed timestep size.

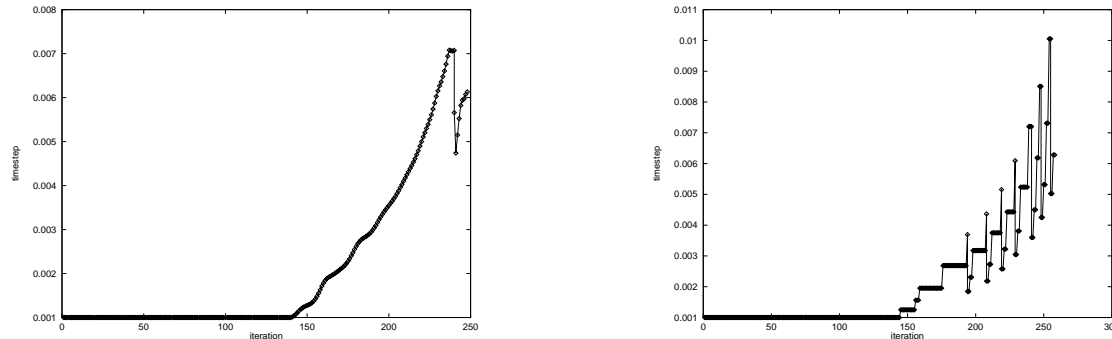| Case	$ntstep$	$nrejec$	nsa	c_{effort}
Fixed Δt	513	0	1547	1
PID Control	248	1	983	0.63
Winget & Hughes	258	7	1045	0.67

Figure 4: Timestep variation using the PID controller (left) and Winget and Hughes approach (right) for $Pr = 0.72$, $Ra = 30000$ in a container with aspect ratio 4:1.

flat free surface, $Ra = 10^3$, $Pr = 0.71$, and Ma = -100. The approximate steady-state velocities and temperature are calculated using biquadratic elements in a uniform mesh with size $h = \frac{1}{16}$. Figure 5 shows the computed stream function and temperature contours, and the effect of the surface tension can be observed. The streamlines are concentrated near the top boundary as similar experiments presented in [10].
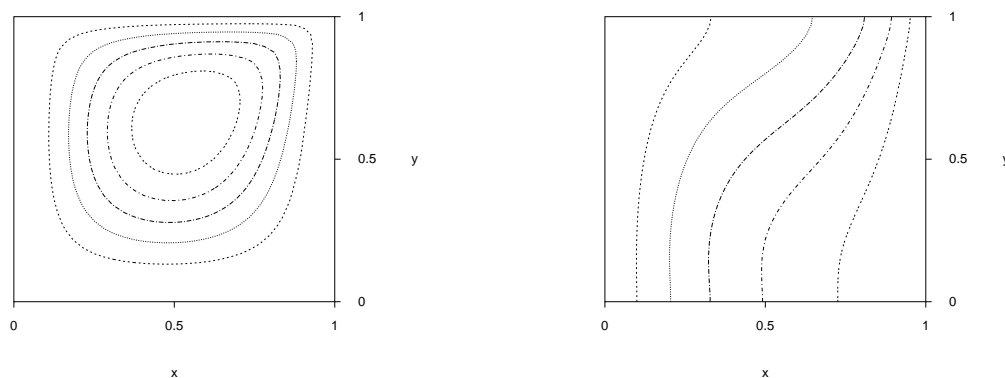

Figure 5: Stream function contours (left) and temperature contour (right) for $Ra = 10^3$, Pr = 0.71, and Ma = -100

To study the behavior of the PID timestep selection, we start with a timestep size of 0.001, the maximum step for which the successive iterations converge. We allow minimum and maximum time steps of 0.001 and 0.1, respectively, and $\tau_u = \tau_T = 10^{-04}$. The solutions are obtained with a tolerance of 0.018 for changes in nodal velocities and 0.01 for changes

in the nodal temperature. The PID parameters are $k_p = 0.01, k_i = 0.55$ and $k_d = 0.01$. As we can see in Table 4, we obtain the solutions with 233 successive approximation iterations using the PID controller. With a fixed timestep size of 0.001, we need 571 iterations. Thus, the solutions are obtained 2.5 times faster using the PID controller. Figures 6 shows the timestep size against time using the PID controller and the Winget and Hughes approach.

Table 4: Results using the PID control and the fixed timestep size when $Pr = 0.71$, $Ra = 1000$ and $Ma = $ -100 in a unit square.

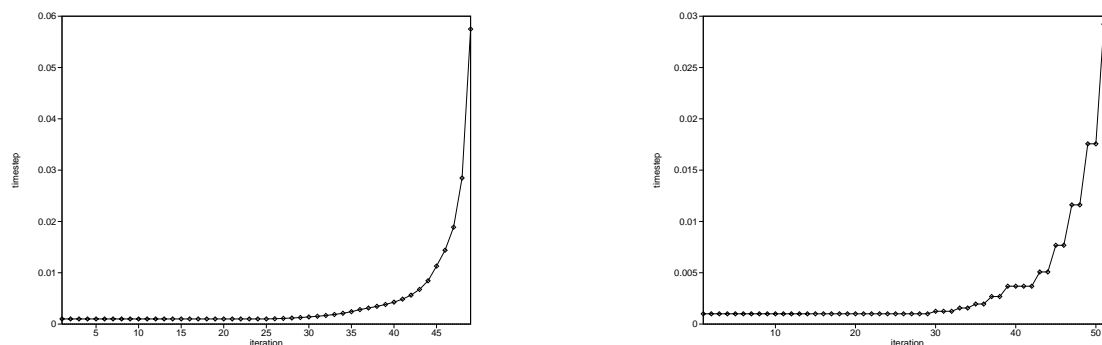| Case	$ntstep$	$nrejec$	nsa	c_{effort}
Fixed Δt	151	0	571	1
PID Control	49	0	233	0.41
Winget & Hughes	52	0	245	0.43

Figure 6: Timestep variation using the PID controller (left) and Winget and Hughes approach (right), $Ra = 10^3$, $Pr = 0.71$, and $Ma = $ -100

5. CONCLUSIONS

We introduce an adaptive timestep selection scheme based on feedback control theory to increase the robustness of our finite element formulation of coupled incompressible viscous flow and transient heat transfer. The finite element flow formulation is based on a penalty Galerkin method and the heat equation utilizes a Galerkin approach. The algorithm employs an iteratively decoupled scheme in the present work.

We solve Rayleigh-Benard-Marangoni problems, and results are compared with fixed timestep, an adaptive timestep scheme from the literature, and our PID control approach. With the PID control strategy we find approximate solutions with a much smaller number of steps without any significant loss of accuracy. For instance, we have a 2.45 times improvement in the computational effort to compute the solution within the same accuracy in the third experiment involving the Marangoni effects. The PID control shows better

results than Winget and Hughes approach in all cases studied here. Our results with PID control for timestep selection show a smooth variation of timesteps, suggesting that a robust algorithm, without heuristics, is possible.

Future numerical experiments involve the calculation of the kinetic energy to improve timestep selection. The nondimensional kinetic energy is a suitable parameter for monitoring the behavior of the liquid phase and for constructing bifurcation diagrams when time progress. The measure of the change over a timestep of the quantities of interest will be defined by the normalized changes in nodal velocities and temperatures, and the nondimensional kinetic energy.

REFERENCES

[1] G.F. Carey, C. Harlé, R. Mclay, and S. Swift. MPP solution of Rayleigh-Benard-Marangoni flows. In *Supercomputing 97*, pages 1–13, San Jose, CA, 1997.

[2] G.De Vahl Davis. Laminar natural convection in a enclosed rectangular cavity. *Int.J. Heat Mass Transfer*, 11:1675–1693, 1968.

[3] G.De Vahl Davis. Natural convection in a square cavity: A comparison exercise. *Int.J.Num.Meth.Fluids*, 3:227–248, 1983.

[4] G.De Vahl Davis. Natural convection of air in a square cavity: A benchmark numerical solution. *Int.J.Num.Meth.Fluids*, 3:249–264, 1983.

[5] M. Griebel, T. Dornseifer, and T. Neunhoeffer. *Numerical Simulation in Fluid Dynamics - A Practical Introduction*. SIAM, Philadelphia, PA, 1998.

[6] K. Gustafsson, M. Lundh, and G. Söderlind. A PI stepsize control for the numerical solution for ordinary differential equations. *BIT*, 28:270–287, 1988.

[7] E. Hairer and G. Wanner. *Solving Ordinary Differential Equations II: Stiff and Differential-Algebraic Problems*. Springer–Verlag, 1993.

[8] A.M.P. Valli, G.F. Carey, and A.L.G.A. Coutinho. Finite element simulation and control of nonlinear flow and reactive transport. In *Proc. 10th Int. Conf. Finite Element in Fluids*, pages 450–455, Tucson, Arizona, 1998.

[9] J.M. Winget and T.J.R. Hughes. Solution algorithms for nonlinear transient heat conduction analysis employing element-by-element iterative strategies. *Comp. Meth. Appl. Mech. and Eng.*, 52:711–815, 1985.

[10] A. Zebib, G.M. Homsy, and E. Meiburg. High marangoni number convection in a square cavity. *Phys. Fluids*, 28(12):3467–3476, 1985.